ROTATIONAL ACCELERATION MEASUREMENT FOR PEDESTRIAN HEAD IMPACT

ROTATIONAL ACCELERATION MEASUREMENT FOR PEDESTRIAN HEAD IMPACT

P. Glay, A. Scattina, M. Avalle

Dipartimento di Ingegneria Meccanica ed Aerospaziale, Politecnico di Torino, Italy

Corresponding author: Alessandro Scattina, Dipartimento di Ingegneria Meccanica e Aerospaziale, Politecnico di Torino, Corso Duca degli Abruzzi, 24 – 10129 Torino Italy

Phone +39-011-0906913

Fax +39-011-0906999

E-mail: alessandro.scattina@polito.it

ROTATIONAL ACCELERATION MEASUREMENT FOR PEDESTRIAN HEAD IMPACT

ABSTRACT

Nowadays, a key point in automotive design is the protection of the Vulnerable Road Users (VRUs), pedestrians and cyclists. Usually, to measure the injuries caused to the head by an impact between a pedestrian and a vehicle, the Head Injury Criterion (HIC) is used. However, this parameter only considers the linear accelerations of the head, while it has been demonstrated that the rotational accelerations are also quite important for the occurrence of damage of the head. From that perspective, this paper investigates in more detail the measure of the rotational accelerations obtained with a special experimental equipment developed by the authors to perform head impact tests, on steel and aluminium bonnets. This data was then looked into to find the influence of some of the physical parameters involved in the rotational accelerations. The results of this study show which parameters have to be taken into particular consideration in the experimental tests. Furthermore, working on these parameters in the design phase can help to reduce injuries to the head for pedestrians.

KEYWORDS: pedestrian protection; rotational acceleration; head injuries evaluation; sensitivity analysis; FE simulation

1. Introduction

Nowadays, one of the key stakes in automotive design is safety. Road traffic accidents are the most important cause of all injuries worldwide [37]. In particular the percentage of VRUs (pedestrians and cyclists) involved in road traffic deaths is very high [37]; and even if the total number of pedestrian fatalities has decreased along the years, when considering the pedestrian fatalities as a proportion of all road traffic fatalities, this number has seen a slight increase in the recent years [12]. Moreover, of all the different categories of people injured, pedestrians bring the highest social costs [12].

In general, when the impact between a pedestrian and a vehicle is studied, the injuries to the legs and to the head are primarily considered [10, 11]. The injuries to the head are usually more severe than the

injuries to the leg [17]. The head injuries are mainly measured with the HIC [6, 32]. However the HIC is often criticized because it is only based on the translational acceleration of the head and does not take into account the rotational accelerations [16, 29]. Indeed, it has been repeatedly shown that the rotational accelerations also contribute to the brain injuries [19-20, 26]. For this reason, alternative injury criteria have been suggested [7, 33] that take into account the measurement of the rotational accelerations of the head.

In accordance with the homologation requirements [11] and with the rating tests [10] for Europe, the pedestrian head is simulated with a headform, made of an aluminium semi-sphere covered by a layer of silicone rubber. The transducers for the measurement of the accelerations are positioned inside the headform. However, different works [18, 22-25] have demonstrated that the head accelerations are heavily influenced by the presence of the neck and by the forces that it can generate during the impact of the head. For this reason, an innovative experimental equipment has been proposed [5, 21], characterized by the presence of a neck simulacrum. Usually the neck part of the Hybrid III dummy is fixed to the traditional headform.

Different solutions to measure the kinematics of the head, and consequently the rotational accelerations have been suggested [2-4, 8-9, 13-15, 27-31, 34-36, 39]. From a theoretical point of view, to determine the kinematics of a six degree of freedom rigid body six accelerometers are sufficient. Indeed, this method is used in several studies [2, 13-15]. However, in order to avoid the unstable computational procedure needed when six accelerometers are used, alternative solutions have been suggested: in [22] a method with nine accelerometers in a 3-2-2-2 array was used or a 3-3-3 array in [34]. An in line accelerometer package using 15 accelerometers [39] or a multi-accelerometer approach using 12 accelerometers [4] were also proposed. A mixture of accelerometers and rate sensors were also used in other solutions [28, 30-31]. A system where three tri-axial accelerometers are positioned inside the headform used for the pedestrian impact tests was also used by the authors of this paper [1]. In this case too, the accelerometers were used to evaluate the rotational accelerations. All the methods discussed up to now can be applied to the headform for the pedestrian head impact test or to the head of a complete dummy or to other similar simulacrum used for this type of test.

This paper describes how, starting from the experimental results obtained by the authors in [1], the measure of the rotational accelerations was investigated by means of a numerical finite element (FE) model. The effects of a set of physical parameters, which can influence this measure, were examined. In the first part of the work the development and tuning through experimental results of a numerical model of the vehicle will be reported. The second part presents the study of the influence of a set of physical parameters which characterize the experimental test, using the numerical model that was developed.

2. Experimental results

As briefly discussed in the introduction, the authors have previously developed an experimental equipment to perform pedestrian head impact tests [1]. In particular, a launching equipment and a specific headform was built. With this headform it is possible to measure not only the linear accelerations but also the rotational ones, by properly placing three triaxial accelerometers inside it. This measuring device can be generally applied not only to the standard headform but also to modified solutions (where, for example, a neck simulacrum is applied) or to the head of a complete dummy. With this equipment, the authors carried out a series of experimental tests of head impacts against the bonnet of a mid-size car (classified into the *Large Family Cars* Euro NCAP category or D-segment EEC 4064/89). Two different types of bonnet were considered: the normal production bonnet made of steel, and a prototype alternative bonnet made of aluminium. In those tests, the linear acceleration, the HIC_{15}, and the rotational accelerations in eight different impact points (Figure 1) were evaluated and discussed. The positions of the impact points were chosen so as to match the stiff components in the engine compartment: the cylinder head, the battery, the fuse box, the lock device, the light device supporting beam and the fender bracket. At least three different bonnets were used in the experimental tests to avoid influences in the test results. The numbering of the impact points is not sequential because this study is part of a more complete work for which a higher number of impact points were considered. In this paper, only the most significant impact points are considered.

3. FEM simulation of experimental tests

A finite element (FE) model of the experimental set-up adopted in [1] was developed. For this application the LS-DYNA® 971 software was used. The FE model consisted of the vehicle and the headform. The FE vehicle model was obtained from a full vehicle model previously developed in Pam-Crash and translated in LS-DYNA®. As usual for this type of applications, only the front part of the vehicle was used. The full vehicle model was trimmed with a plane perpendicular to the X axis of the vehicle at the lower border of the windshield. The components of the vehicle involved in the pedestrian head impact were then meshed with higher accuracy than the original model.

With this FE model, the head impact tests were simulated and results obtained for all the impact points considered (Figure 1). To improve the suitability of the FE model, both the steel and the aluminium bonnet were simulated. The evaluated performance were the HIC_{15} (1), the linear acceleration in the centre of gravity of the headform, and the rotational accelerations of the headform around the *y* axis (Figure 2). Only this component of the rotational accelerations was considered because, as discussed in [1], it is the most important and significant. As well known, HIC is defined as:

$$HIC = \max\left[\frac{1}{t_2 - t_1}\int_{t_1}^{t_2} a(t)dt\right]^{2.5}(t_2 - t_1) \qquad (1)$$

The simulation results are summarized in Table 1 where the numerical and experimental HIC_{15} results are compared and in Figures 3-6 where the linear and rotational accelerations are examined. All the acceleration signals were filtered with the SAE 600 filter. Examining the values of the HIC_{15}, the agreement between the experimental and numerical results is good in some impact points while in other points, such as P6, P9, P10 the difference is important. Considering the position of the impact points (Fig. 1), the differences between the numerical and experimental results can be due to how some parts in the engine compartment were modelled. For example, at point P6, the bonnet hits the lock device, which is modelled in a simplified way: since the HIC_{15} is highly susceptible to small variations, these small simplifications can have important effects on the result. At points P2 and the P3 the agreement is very good both in terms of HIC_{15} values and time interval, whereas at point P4 the model is predictive apart from an additional peak at around 7 ms: at this time, the bonnet comes into contact with the upper

components of the engine compartment. For the aluminium solution as well, the second part of the curve, starting from around 7-8 ms, is not representative of the experimental result. This behaviour can again be explained by a lack of detailed modelling of some of the components inside the engine compartment. It is interesting to notice that for the steel solution at point P6 there is a better global match of the curves than in the aluminium bonnet: however, the difference in the HIC values are higher in the case of the steel solution. This is clearly because the exponent 2.5 in the HIC expression is strong in highlighting even small differences. At point P7 instead, the numerical and experimental curves and HIC_{15} are in good agreement. Examining points P9, P10 and P11, the match is good, in particular for the steel version and the first peak is always higher in the numerical models: this can be due to a difference between the battery used in the FE model and the one in the real vehicle, which could not be modelled correctly in more details.

To sum up, in most cases the FE model reproduces the experimental results well and the differences can be explained by the incomplete modelling of some components in the engine compartment. In fact, it was not possible to describe these components better due to a lack of more precise information.

Moreover, dynamic impact simulations are strongly non-linear, consequently small uncertainties in the boundary conditions can give large scatter in the results. Not necessary a more detailed numerical model could give better results.

Finally, to complete the validation of the numerical model, the rotational acceleration around *y* axis also was considered. Examining the curves shown in Figs. 4-6, it is clear that the correlation is far from being acceptable for all the considered impact points. The FE model is not representative of the experimental results concerning the rotational accelerations.

4. Sensitivity analysis

In order to minimize the error between the experimental and the numerical simulation results, in particular concerning the rotational accelerations, the effect of the different numerical parameters on the numerical results was examined. In particular the effect of different types of contact formulation, element formulation and mesh quality were investigated. However, the influence of these simulation parameters proved to be negligible.

Subsequently, the effect of some physical parameters was studied. These parameters have measurement uncertainties and are worth investigating both considering a traditional headform or a modified one, where also the neck is considered. In particular, the following parameters were examined:

- Headform impact speed
- Headform impact angle
- Position of the reference system of the accelerometers
- Friction coefficient between the headform and the bonnet surface

The study was carried out first with simple numerical simulations where each single parameter was modified. When a given parameter seemed to change the results considerably, it was analysed more in depth, with a sensitivity analysis. The influence of the different parameters is discussed in details in the following paragraphs. Moreover, for the most influencing parameter, an optimization process was also carried out in order to find the optimal value to match the numerical and the experimental results.

4.1 Impact speed

The influence of the impact velocity of the headform was first considered. The simulations referred to the nominal value of 40 km/h. However, during the experimental tests, at the time of the impact, the speed of the headform can be slightly different; a scatter of 5% with regards to the nominal speed was measured. For this reason, a numerical simulation with a difference of 5% in the initial velocity of the headform was performed. The results obtained in terms of HIC_{15}, linear and rotational acceleration curves, varied less than 1%. Hence, it is possible to conclude that a small variation of this parameter does not affect the phenomenon.

4.2 Impact angle

During the experimental test, before the impact with the bonnet, the headform is in free flight. During the shot of the headform, the launch equipment suffered a slight rotation due to the bending of its main supporting beams. This can cause the trajectory of the headform to change slightly during the free flight. It introduces a small variation in the impact angle between the bonnet and the headform. Consequently, the impact location is slightly different from test to test. For some impact points, this difference in the position can produce important changes in the results. To study the influence of this parameter,

simulations were carried out with a different impact angle. Specifically, the initial value of 40° was changed by ±1° and then by ±5°. Both the linear (Figure 7) and the rotational accelerations (Figure 8) were taken into consideration. The results show that the impact angle had no influence on the linear accelerations, at least in the range of variation considered. However, a certain influence can be noticed on the rotational accelerations. The first peak of the curve is not affected by the variation of the impact angle, but the behaviour after this first peak, in the interval from 4 to 12 ms, changes significantly.

4.3 Position of the reference system of the accelerometers

As it was explained before, the headform can undergo slight variations with respect to its nominal trajectory. For example, when the headform is fixed on the launching equipment, its position can deviate from the theoretical position [1]. This means that the nominal position of the reference systems of the accelerometers inside the headform is not as expected. The influence of this positioning error was investigated. Different cases were evaluated by rotating the reference systems of the accelerometers around their local *z* axis:

- a single reference system is rotated while the other two are in the correct position;
- two reference system are rotated of the same amount while the third one is in the correct position;
- all three reference systems are rotated of the same amount.

For the three cases a rotation of 1° was considered, since no bigger variation is expected. Only the influence on the rotational acceleration was examined because the three accelerometers are required just for this measurement, while for the linear acceleration only one accelerometer is used. As it is possible to see in Figure 9, the rotation of the local reference systems of the accelerometers does not influence the evaluation of the rotational acceleration. The few differences between the curves can be accounted by numerical instabilities.

4.4 Friction coefficient between the headform and the bonnet surface

The influence of the friction coefficient between the bonnet surface and the headform was evaluated with a sensitivity analysis using the LS-OPT software [38]. The friction coefficient depends on many circumstances, such as the materials of the bodies in contact, the strain rate, the thermal conditions, etc. Starting with the nominal value of 0.2, used in the first simulations reported in section 3, the sensitivity

analyses were carried out by using the Monte Carlo method [38]. At this stage, only the influence on impact point P7 of the steel bonnet was evaluated. The reason is that for this solution, the difference in this point between the numerical and the experimental results is negligible. Moreover, this point is more or less in the middle of the bonnet surface, so the possible influence of the surrounding structures is small. Different ranges of friction coefficient were tested, starting from 0.07 to 0.55. In Figure 10 and 11 the influence of this parameter on the linear and the rotational accelerations respectively is shown. Concerning the linear acceleration, the main influence is on the first peak of the curve; then the curves have quite the same behaviour: the higher the friction coefficient, the higher the peak. This can probably be explained by a less slipping for the headform when the friction coefficient is higher. Concerning the rotational acceleration, the influence is not only on the intensity of the first peak but also heavily on the behaviour in the second part of the curve. With a small variation in the friction coefficient, the curve's trend may change considerably and the behaviour gets closer to the experimental results.

5. Optimization analysis

The sensitivity analysis highlighted that the most influencing physical parameter of the pedestrian head impact test is the friction coefficient between the headform and the bonnet surface. For this reason a parameter optimization concerning this factor was carried out. The final objective was to minimize the error between the experimental and the simulation results in order to set-up the FE model.

This non-linear optimization process is usually applied to identify the material parameters starting from experimental results. The software LS-OPT generates the numerical curve and tries to match it with the experimental one, i.e. to minimize the error between the two curves.

In this study, the optimization analysis aimed at identifying the friction f between the bonnet and the headform. In this type of problem, the static and dynamic coefficients of friction can be considered the same. The initial value for the coefficient of friction f was set to 0.2. Three different head impact points (P6, P7, P9) were considered in order for the results to be independent of the impact location. In addition, this allowed for more accurate results.

The optimization was based on three experimental results: the HIC_{15} value, the linear acceleration and the rotational acceleration along the y axis of the headform. It is thus a multi-objective problem but

because the HIC_{15} value depends on the linear acceleration, the weight of the first two objectives was arbitrary chosen half the weight applied to the rotational acceleration.

To evaluate the difference between the experimental and the numerical results the curve mapping approach was used [38]. The principle of this error measurement is to create a surface between the experiment and numerical curve. Next the algorithm cuts this surface in subdomains and tries to reduce every area. The optimization is not directly made on the numerical model responses but based on an interpolated surface, called the metamodel. The metamodel is an approximation of the system responses. The radial basis function was chosen for the metamodel [38]. It helps get a good overview and approximate non-linear responses without being too time-consuming. With this optimization process, a friction coefficient of 0.23 was identified.

Finally, the head impacts on all the points were simulated again with the identified friction coefficient. The results are summarized in Table 2, in terms of HIC, and in Figure 12 and 13 in terms of the linear and rotational accelerations at some impact points. As expected, there was a slight increase of all the response values concerning the HIC_{15}. The increase in the friction coefficient brings an increase of the first peak of the linear acceleration curves, and, consequently, the HIC is also higher. Considering the linear accelerations, no particular effects were observed. However, it is interesting to note that, for all the impact points, the rotational accelerations match better with the experimental results.

6. Conclusions

This study examined the influence of some physical parameters on the measurement of the linear and rotational accelerations of a headform during a pedestrian head impact against a vehicle front experiment. These measurements are important to evaluate the injuries to the pedestrian's head, in particular for the rotational accelerations. Since, during the impact, the head accelerations are influenced by the forces applied by the neck, similar considerations can be made also for more complex devices, where a simulacrum of the neck is applied to the headform. The work was carried out with a numerical approach, starting from experimental results previously obtained by the authors. The parameters considered were the impact speed, the impact angle, the position of the accelerometers inside the headform and the friction coefficient between the bonnet surface and the headform. Among these, the

most influencing parameters are the friction coefficient, and secondly the impact angle. In order to better reproduce the experimental results, an optimization process was applied to study and identify the friction coefficient. With the identified value of the friction coefficient, there was a much better match between the numerical and the experimental results. These analyses show which parameters should be carefully considered during the experimental tests. However, working on these parameters can also contribute reducing the injuries to the pedestrian's head during an impact.

References

[1] M. Avalle, G. Belingardi and A. Scattina, *Numerical and experimental investigation of a lightweight bonnet for pedestrian safety*, Int. J. of Crash. 18(1) (2013), pp. 29–39.

[2] E. Becker and G. Willems, *An experimentally validated 3-D inertial tracking package for application in biodynamic research*, J. Stapp Car Crash, 19, SAE Paper 751173, SAE International, Warrendale, PA, 1975.

[3] F. Bendjellal, L. Oudenard, E. Eller, M. Koch, I. Planath, and C. Tarriere, *Measurement of head angular acceleration in crash tests: development of an electronic device for the hybrid III dummy*, J. Stapp Car Crash, 36, SAE Paper 922511, SAE International, Warrendale, PA, 1992.

[4] F. Bendjellal, L. Oudenard, J. Uriot, C. Brigout, and F. Brun-Canau, *Computation of hybrid III head dynamics in various impact situations*, J. Stapp Car Crash, 34, SAE Paper 902320, SAE International, Warrendale, PA, 1990.

[5] J. Bovenkerk, C. Sahr, O. Zander and I. Kalliske, *New modular assessment methods for pedestrian protection in the event of head impacts in the windscreen area*, 21st international conference on the enhanced safety of vehicles (ESV), 2009.

[6] C. Chou and G. Nyquist, *Analytical Studies of the Head Injury Criterion (HIC)*, SAE Technical Paper 740082, SAE International, Warrendale, PA, 1974.

[7] C. Deck and R. Willinger, *Improved head injury criteria based on head fe model*, Int. J. of Crashworthiness 13(6) (2008), pp. 667–678.

[8] F.P. Dimasi, *Transformation of Nine-Accelerometer-Package (NAP) Data for Replicating Headpart Kinematics and Dynamic Loading*, NHTSA Technical Report, DOT HS 808 282, 1995.

[9] F.P. Dimasi, R.H. Eppinger, and F.A. Bandak, *Computational Analysis of Head Impact Response Under Car Crash Loadings*, J. Stapp Car Crash, 39, SAE Paper 952718, SAE International, Warrendale, PA, 1995.

[10] European New Car Assessment Programme, Pedestrian testing protocol, Version 7.1.1, December 2013.

[11] European Parliament, Directive 2003/102/EC.

[12] European Road Safety Observation, DaCoTa - Traffic Safety Basic Facts 2012.

[13] C.L. Ewing, D.J. Thomas, L. Lustick, E. Becker, G.C. Willems, and W.H. Muzzy, *The effect of the initial position of the head and neck on the dynamic response of the human head and neck to -Gx impact acceleration*, J. Stapp Car Crash, 19, SAE Paper 751157, SAE International, Warrendale, PA, 1975.

[14] C.L. Ewing, D.J. Thomas, L. Lustick, W.H. Muzzy, G.C. Willems, and P. Majewski, *Dynamic response of the human head and neck to +Gy impact acceleration*, J. Stapp Car Crash, 21, SAE Paper 770928, SAE International, Warrendale, PA, 1977.

[15] C.L. Ewing, D.J. Thomas, P.L. Majewski, R. Black, and L. Lustick, *Measurement of head, T1, and pelvic response to -Gx impact acceleration*, J. Stapp Car Crash, 21, SAE Paper 770927, SAE International, Warrendale, PA, 1977.

[16] F. Feist, J. Gugler, C. Arregui-Dalmases, E. del Pozo de Dios, F. Lopez-Valdes, D. Deck, and R. Willinger, *Pedestrian collisions with flat-fronted vehicles: injury patterns and importance of rotational accelerators as a predictor for traumatic brain injury (tbi)*, 21st international conference on the enhanced safety of vehicles (ESV), 2009.

[17] B. Fildes, H.C. Gabler, D. Otte, and A. Linder, *Pedestrian Impact Priorities Using Real-World Crash Data and Harm*, Ircobi - international research council on the biomechanics of impact conference, Graz, Austria, 2004.

[18] R. Fredriksson, *PRIORITIES AND POTENTIAL OF PEDESTRIAN PROTECTION Accident data, Experimental tests and Numerical Simulations of Car-to-Pedestrian Impacts*, Karolinska Institutet, Stockholm 2011.

[19] T.A. Gennarelli and L.E. Thibault, *Comparison of translational and rotational head motions in experimental cerebral concussion*. 15th Stapp Car Crash Conference, pp. 797–803. Society of Automotive Engineers, Warrendale, PA, 1971.

[20] T.A. Gennarelli, L.E. Thibault, and A.K. Ommaya, *Pathophysiologic responses to rotational and translational accelerations of the head*, 15th Stapp Car Crash Conference, Society of Automotive Engineers, Warrendale, PA, 1972.

[21] R. Hardy, *Final report for the work on "Pedestrian and Pedal Cyclist Accidents" (SP3)*, Aprosys Project, April 2009.

[22] B.J. Hardy, G.J.L. Lawrence, I.M. Knight, I.C.P. Simmons, J.A. Carroll, G. Coley and R.S. Bartlett*, A study of possible future developments of methods to protect pedestrians and other vulnerable road users*, project report UPR/VE/061/07, TRL Limited, 2007.

[23] J. Kerrigan, C. Arregui and J. Crandall, *Pedestrian head impact dynamics: comparison of dummy and PMHS in small sedan and large SUV impacts*, 21st international conference on the enhanced safety of vehicles (ESV), 2009.

[24] J. Kerrigana, C. Arregui-Dalmasesab and J. Crandalla, *Assessment of pedestrian head impact dynamics in small sedan and large SUV collisions*, Int. J. of Crash. 17(3) (2012), pp. 243–258.

[25] J. Kerrigan, J. Crandall and B. Deng, Pedestrian kinematic response to mid-sized vehicle impact. Int. J. of Vehicle Safety 2(3) (2007), pp. 221–240.

[26] S. Kleiven, *Predictors for traumatic brain injuries evaluated through accident reconstructions*, 51st J. Stapp Car Crash, SAE International, Warrendale, PA, 2007.

[27] K.W. Krieger, A.J. Padgaonkar, and A.I. King, *Full-scale experimental simulation of pedestrian-vehicle impacts*, J. Stapp Car Crash 20, SAE Paper 760813, SAE International, Warrendale, PA, 1976.

[28] D.R. Laughlin, *A magnetohydrodynamic angular motion sensor for anthropomorphic test device instrumentation*, J. Stapp Car Crash, 33, SAE Paper 892428, SAE International, Warrendale, PA, 1989.

[29] D. Marjoux, D. Baumgartner, C. Deck, R. Willinger, *Head injury prediction capability of the HIC, HIP, SIMon and ULP criteria*, Accident Anal. Prevention 40(3) (2008), pp. 1135–1148.

[30] P.G. Martin, ,G.W. Hall, J.R. Crandall, and W.D. Pilkey, *Measuring the Acceleration of a Rigid Body*, Shock and Vibration 5 (1998), pp. 211–224.

[31] P.G. Martin, G.W. Hall, J.R. Crandall, W.D. Pilkey, C.C. Chou, and B.B. Fileta, *Measurement Techniques for Angular Velocity and Acceleration in an Impact Environment*, SAE Paper No. 970575, SAE International, Warrendale, PA, 1997, pp. 49–54.

[32] J. McElhaney, *Head injury criteria*, Polymer Mechanics 12(3) (1976), pp 411–429.

[33] J. Newman, *A generalized acceleration model for brain injury threshold (GAMBIT)*, IRCOBI Conference, Zurich, Switzerland, 1986.

[34] G.S. Nusholtz, *Geometric Methods in Determining Rigid-body Dynamics*, Experimental Mechanics 33 (1993), pp.153–158.

[35] G.S. Nusholtz, P.S. Kaiker, and R.J. Lehman, *Critical limitations on significant factors in head injury research*, J. Stapp Car Crash, 30, SAE Paper 861890, SAE International, Warrendale, PA, 1986.

[36] A.J. Padgaonkar, K.W. Krieger, and A.I. King, *Measurement of Angular Acceleration of a Rigid Body Using Linear Accelerometers*, J. Applied Mechanics 42 (1975), pp. 552–556.

[37] M. Peden, R. Scurfield, D. Sleet, D. Mohan, A.A. Hyder, E. Jarawan and C. Mathers, *World report on road traffic injury prevention*, World Health Organization, Geneve, 2004.

[38] N. Stander, W. Roux, A. Basudhar, T. Eggleston, T. Goel and K Craig, *LS-OPT® User's Manual - A design optimization and probabilistic analysis tool for the engineering analyst*, Livermore Software Technology Corporation, Livermore, California, 2013.

[39] D.C. Viano, J.W. Melvin, J.D. McCleary, R.G. Madeira, T.R. Shee, and J.D. Horsch, *Measurement of head dynamics and facial contact forces in the Hybrid III dummy*, J. Stapp Car Crash, 30, SAE Paper 861891, SAE International, Warrendale, PA, 1986.

	STEEL			ALUMINIUM		
	EXPERIMENTAL	FEM	Δ%	EXPERIMENTAL	FEM	Δ%
P2	1909	1754	-8.1	2613	2340	-10.4
P3	1989	1570	-21.1	2324	1986	-14.5
P4	1250	1229	-1.7	1095	774	-29.3
P6	895	1132	26.5	955	981	2.7
P7	1194	1193	-0.1	1529	1619	5.9
P9	679	1158	70.5	644	1098	70.5
P10	875	1308	49.5	1015	1249	23.1
P11	1439	1096	-23.8	1582	1459	-7.8

	STEEL			ALUMINIUM		
	EXPERIMENTAL	FEM	FEM OPTIMIZED	EXPERIMENTAL	FEM	FEM OPTIMIZED
P2	1909	1754	1753	2613	2340	2495
P3	1989	1570	1573	2324	1986	1989
P4	1250	1229	1200	1095	774	940
P6	895	1132	1273	955	981	1151
P7	1194	1193	1211	1529	1619	1651
P9	679	1158	1310	644	1098	1243
P10	875	1308	1514	1015	1249	1478
P11	1439	1096	1124	1582	1459	1356

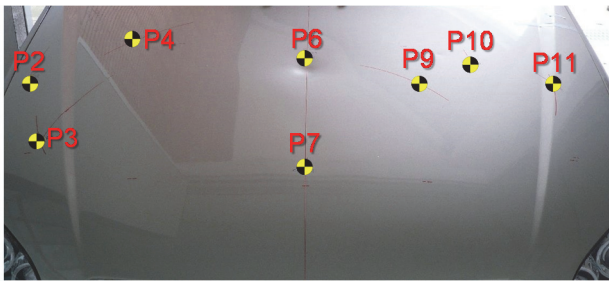

Figure 1: position of the impact points considered on the bonnet surface.

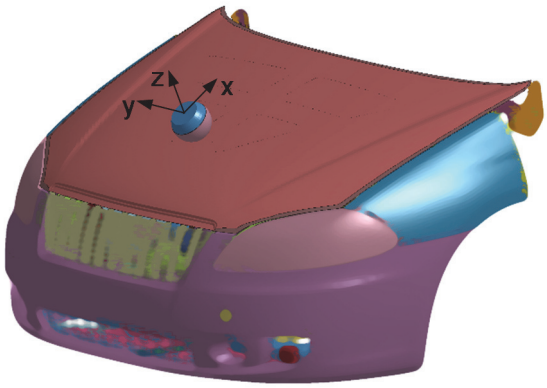

Figure 2: local reference system of the headform.

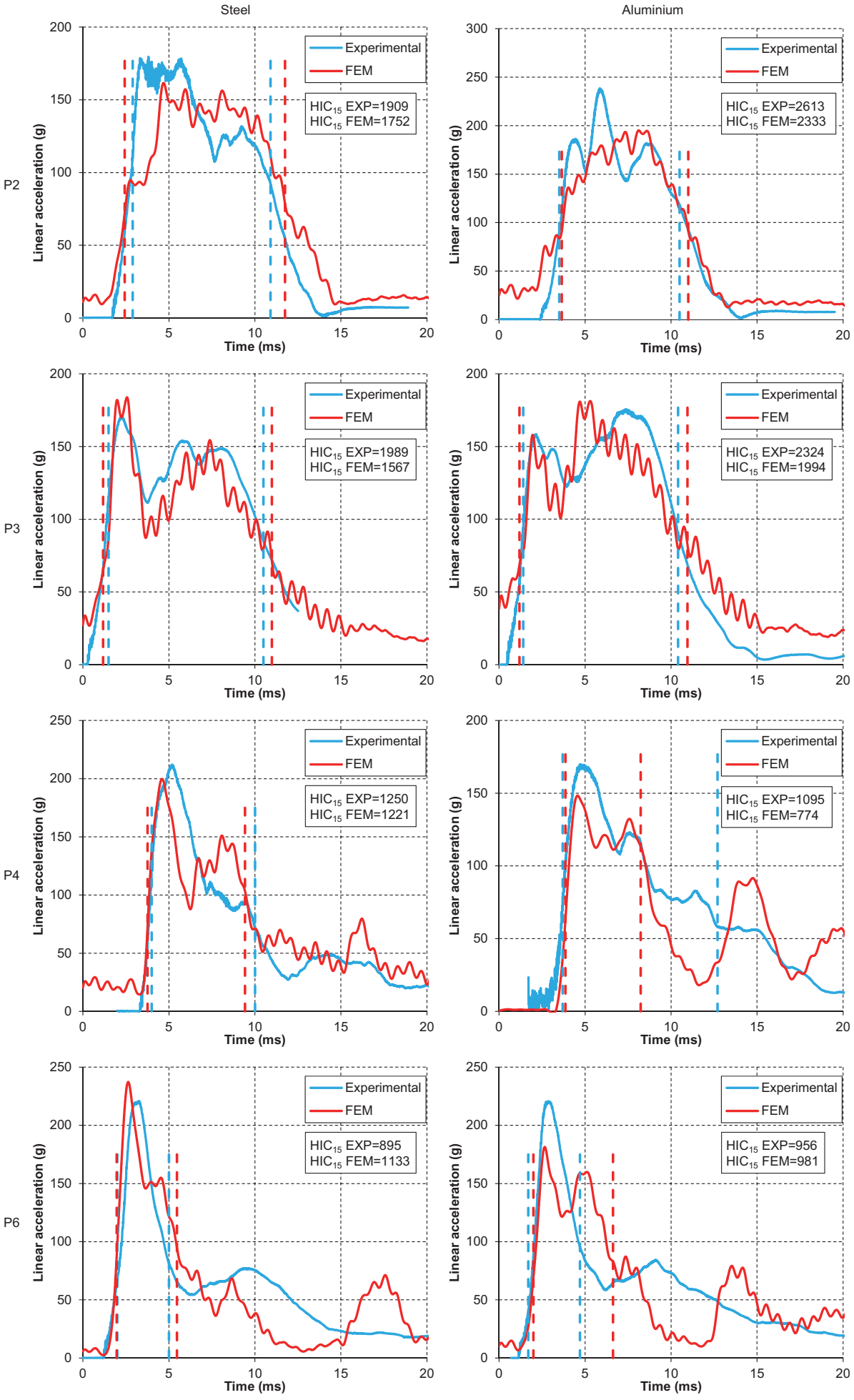
Steel
Aluminium
P2
P3
P4
P6
Experimental
FEM
HIC15 EXP=1909
HIC15 FEM=1752
HIC15 EXP=2613
HIC15 FEM=2333
HIC15 EXP=1989
HIC15 FEM=1567
HIC15 EXP=2324
HIC15 FEM=1994
HIC15 EXP=1250
HIC15 FEM=1221
HIC15 EXP=1095
HIC15 FEM=774
HIC15 EXP=895
HIC15 FEM=1133
HIC15 EXP=956
HIC15 FEM=981
Linear acceleration (g)
Time (ms)

Figure 3: resultant linear acceleration curves in the centre of gravity of the headform: comparison between numerical and experimental results. On the left the results of the impacts on the steel bonnet, on the right the result on the aluminium bonnet. The impact points considered are P2, P3, P4 and P6 (from top to bottom).

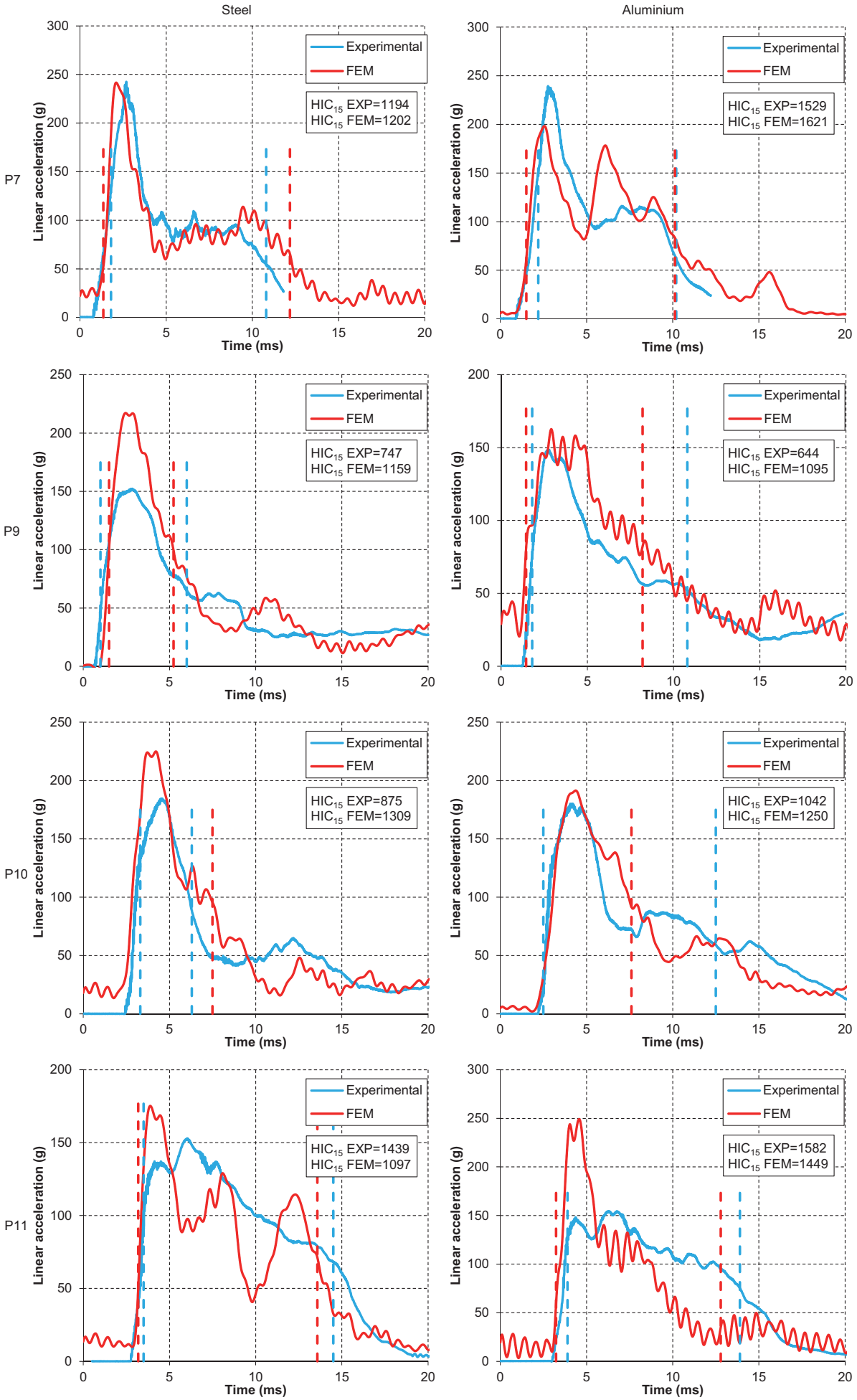
Steel
Aluminium
P7
P9
P10
P11
Experimental
FEM
HIC15 EXP=1194
HIC15 FEM=1202
HIC15 EXP=1529
HIC15 FEM=1621
HIC15 EXP=747
HIC15 FEM=1159
HIC15 EXP=644
HIC15 FEM=1095
HIC15 EXP=875
HIC15 FEM=1309
HIC15 EXP=1042
HIC15 FEM=1250
HIC15 EXP=1439
HIC15 FEM=1097
HIC15 EXP=1582
HIC15 FEM=1449
Linear acceleration (g)
Time (ms)

Figure 4: resultant linear acceleration curves in the centre of gravity of the headform: comparison between numerical and experimental results. On the left the results of the impacts on the steel bonnet, on the right the result on the aluminium bonnet. The impact points considered are P7, P9, P10 and P11 (from top to bottom).

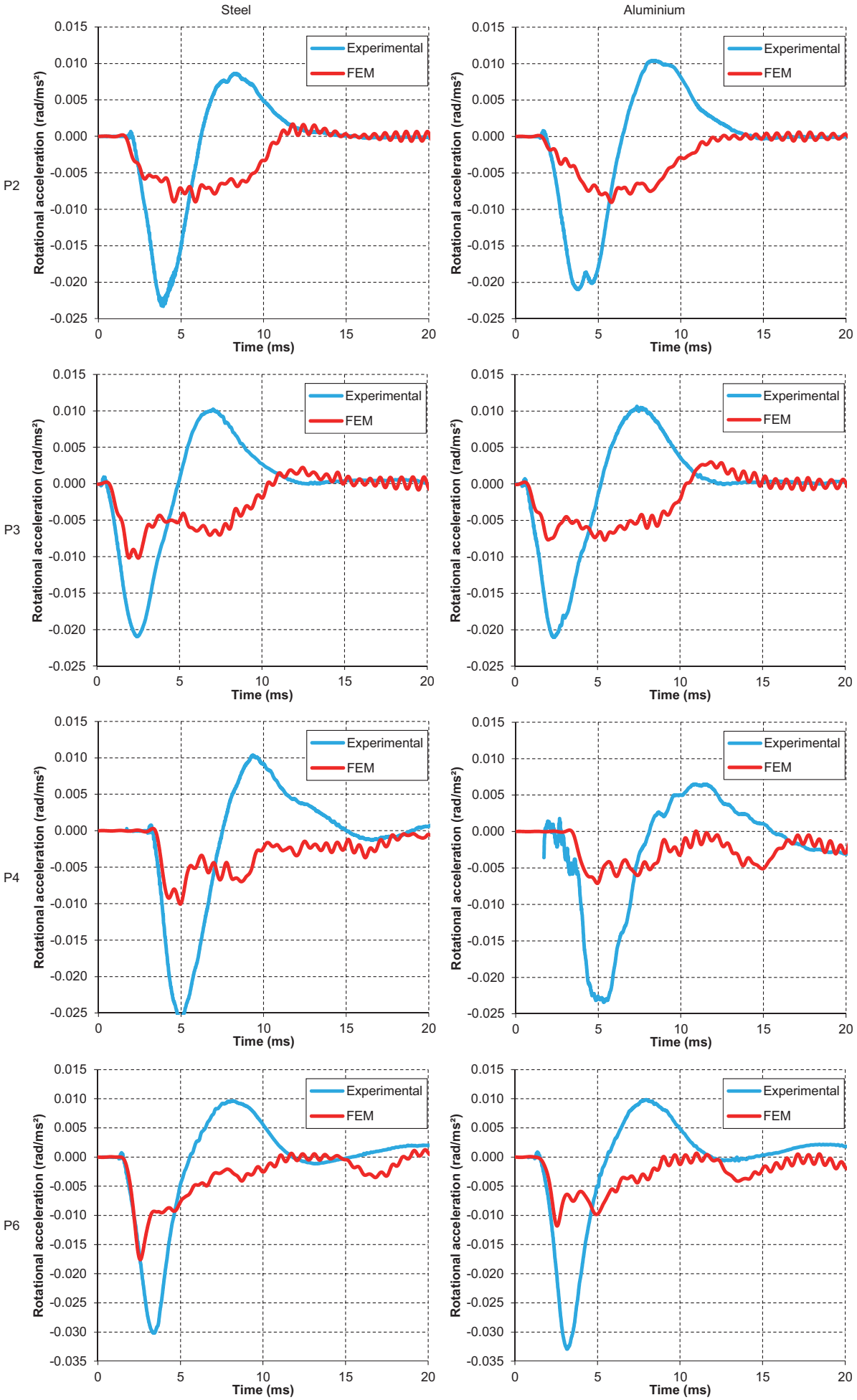
Steel
Aluminium
P2
P3
P4
P6
Experimental
FEM
Rotational acceleration (rad/ms²)
Time (ms)

Figure 5: rotational acceleration curves of the headform: comparison between numerical and experimental results. On the left the results of the impacts on the steel bonnet, on the right the result on the aluminium bonnet. The impact points considered are P2, P3, P4 and P6 (from top to bottom).

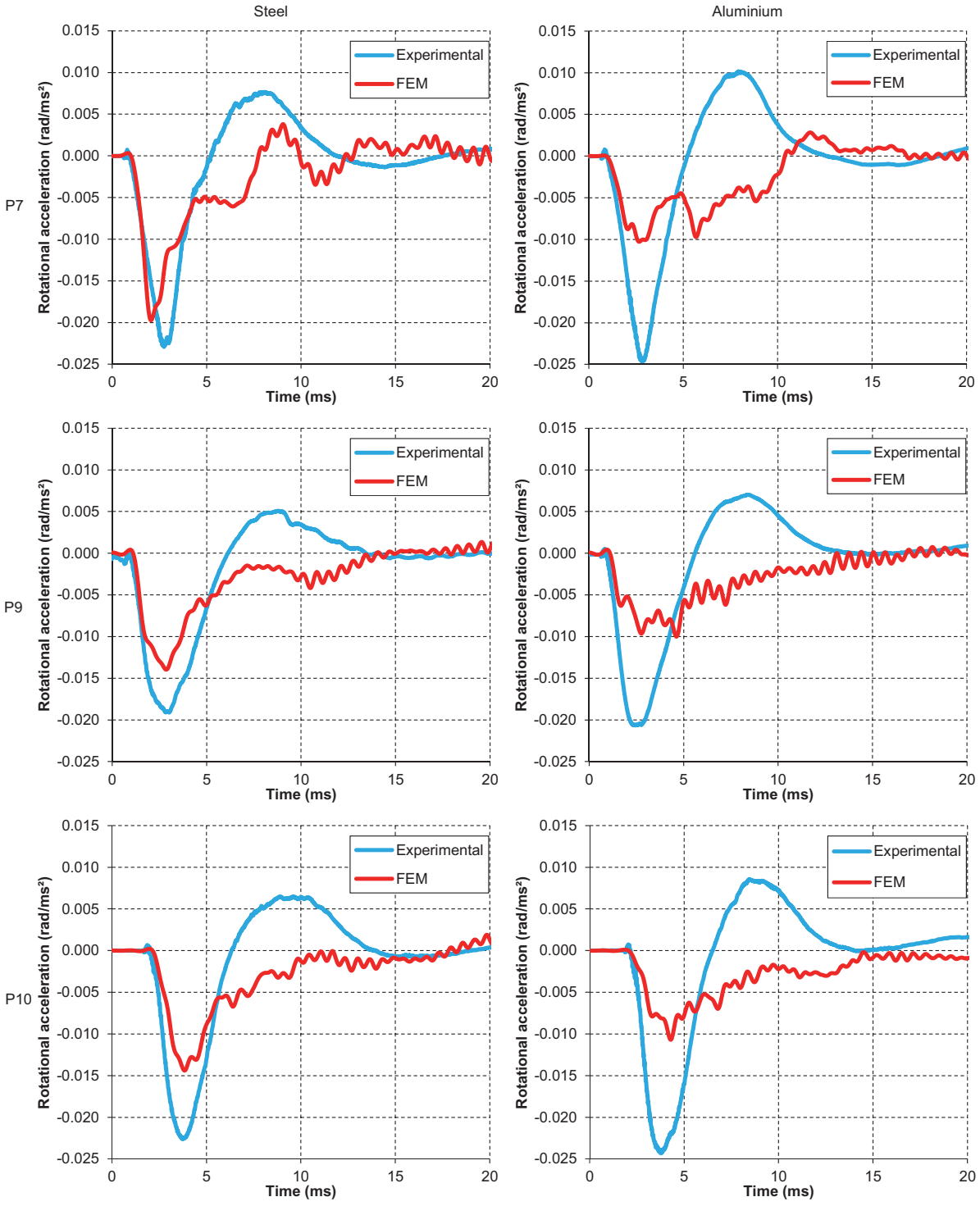

Figure 6: rotational acceleration curves of the headform: comparison between numerical and experimental results. On the left the results of the impacts on the steel bonnet, on the right the result on the aluminium bonnet. The impact points considered are P7, P9, P10 and P11 (from top to bottom).

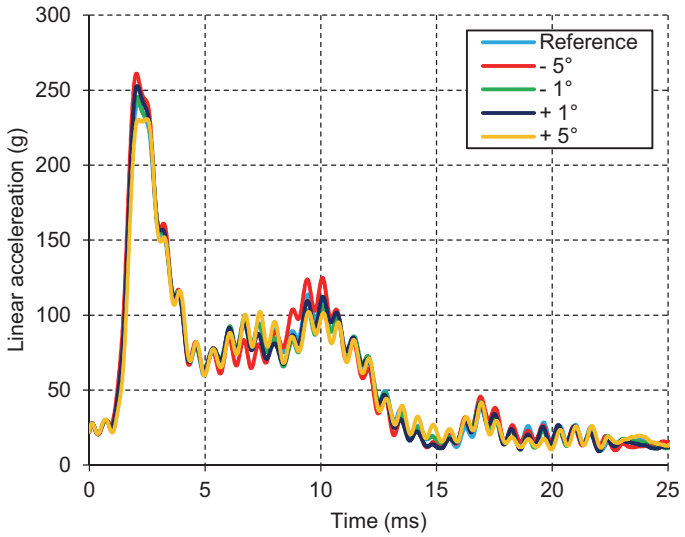

Figure 7: linear acceleration curves in the centre of gravity of the headform: comparison between different impact angles.

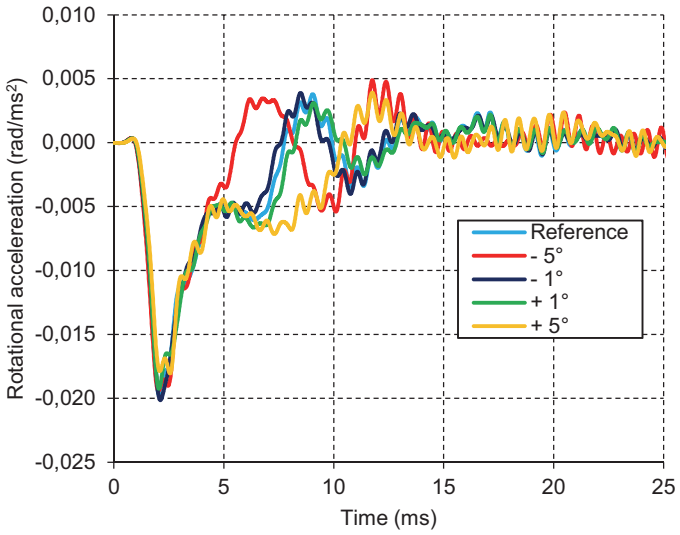

Figure 8: rotational acceleration curves in the centre of gravity of the headform: comparison between different impact angles.

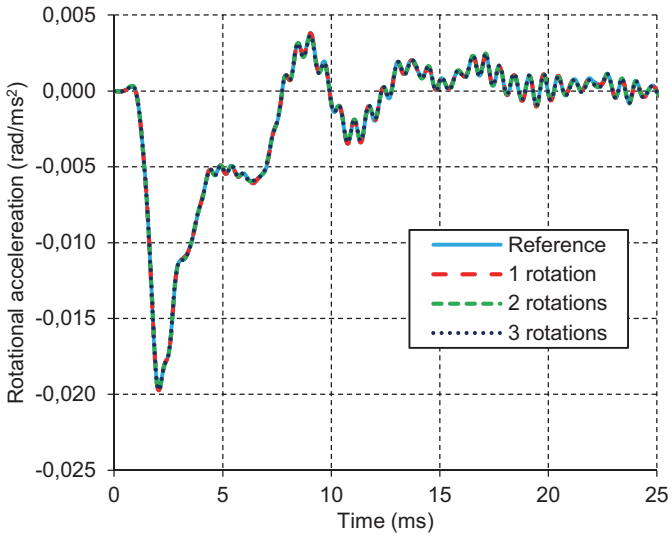

Figure 9: rotational acceleration: influence of the relative position of the reference system of the accelerometers.

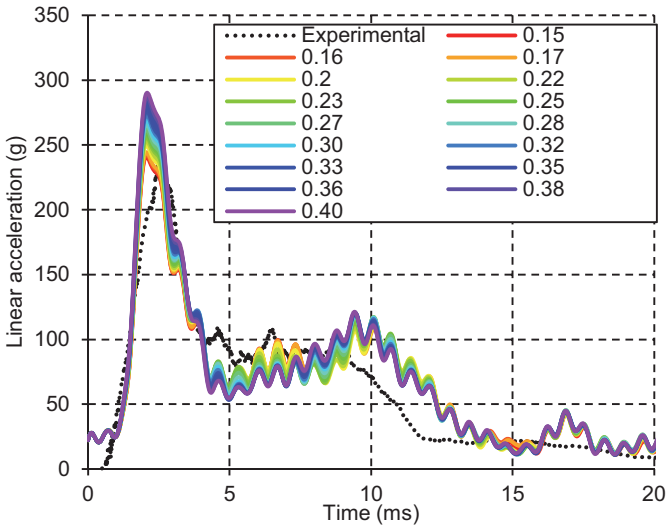

Figure 10: linear acceleration in the centre of gravity of the headform: influence of the friction coefficient.

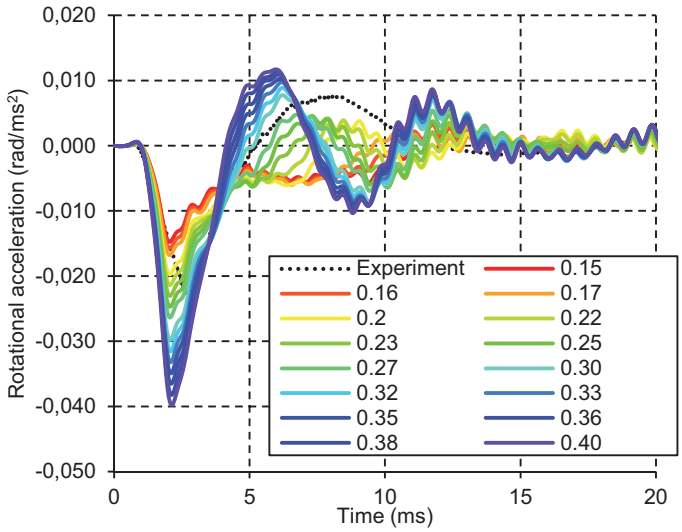

Figure 11: rotational acceleration of the headform: influence of the friction coefficient.

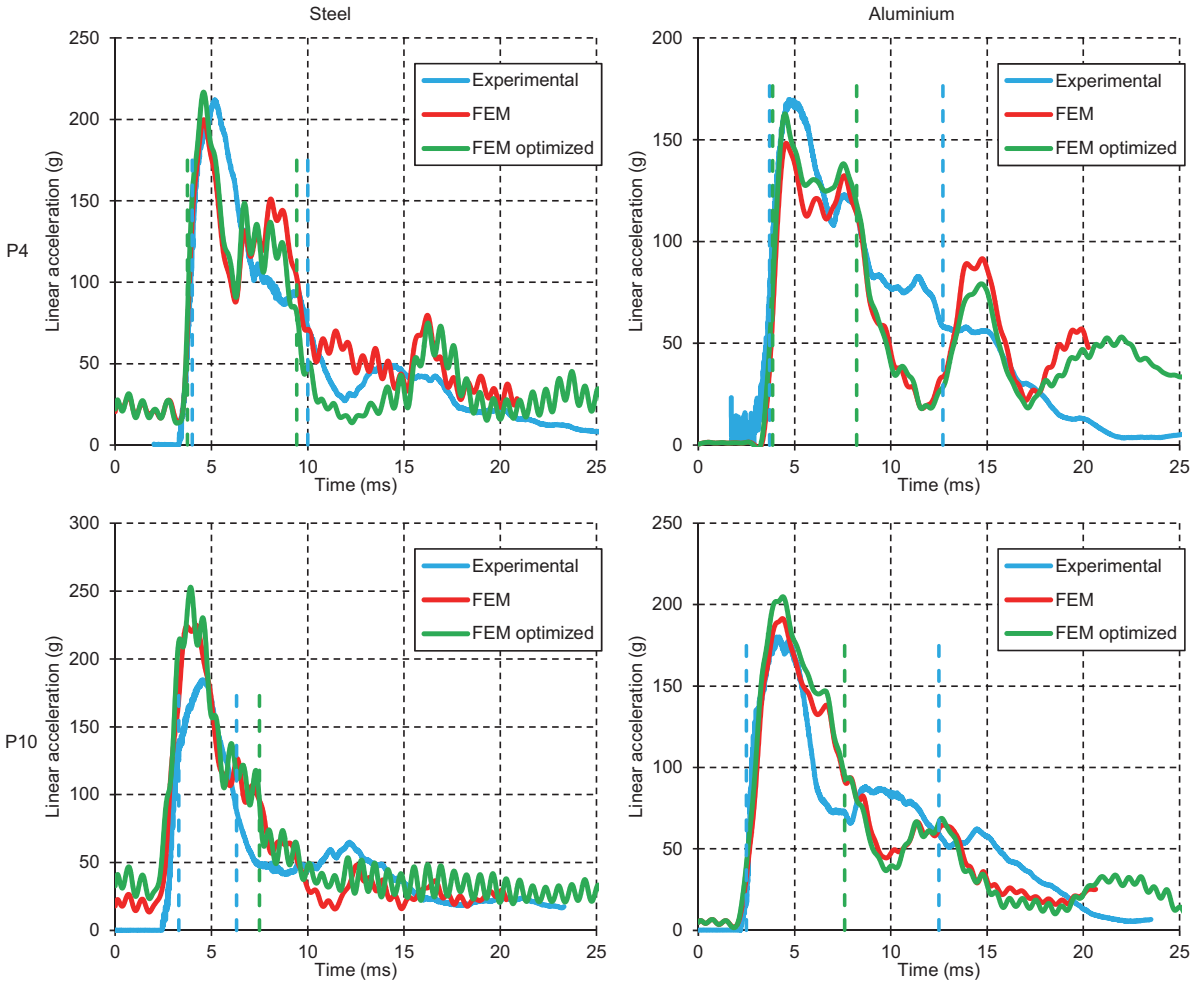

Figure 12: resultant linear acceleration curves in the centre of gravity of the headform: comparison between experimental and numerical results before and after the optimization process. On the left the results of the impacts on the steel bonnet, on the right the result on the aluminium bonnet. The impact points considered are P4, and P11 (from top to bottom).

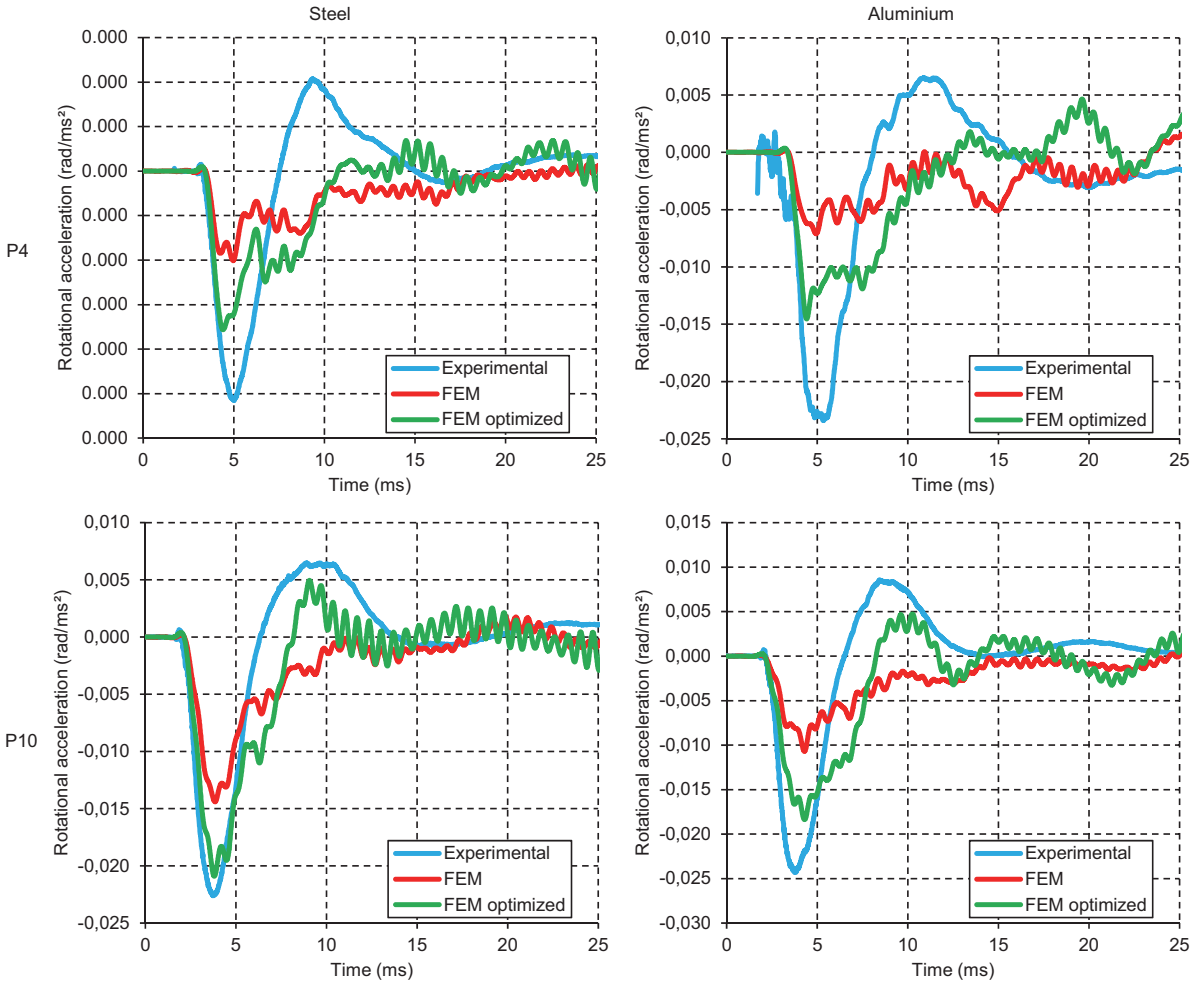

Figure 13: resultant rotational acceleration curves in the centre of gravity of the headform: comparison between experimental and numerical results before and after the optimization process. On the left the results of the impacts on the steel bonnet, on the right the result on the aluminium bonnet. The impact points considered are P4, and P11 (from top to bottom).